Science Advances
AAAS

advances.sciencemag.org/cgi/content/full/6/22/eaaz5858/DC1

Supplementary Materials for

Generation of self-organized sensory ganglion organoids and retinal ganglion cells from fibroblasts

Dongchang Xiao, Qinqin Deng, Yanan Guo, Xiuting Huang, Min Zou, Jiawei Zhong, Pinhong Rao, Zihui Xu, Yifan Liu, Youjin Hu, Yin Shen*, Kangxin Jin*, Mengqing Xiang*

*Corresponding author. Email: xiangmq3@mail.sysu.edu.cn (M.X.); kxjin@yahoo.com (K.J.); yinshen@whu.edu.cn (Y.S.)

Published 29 May 2020, *Sci. Adv.* **6**, eaaz5858 (2020)
DOI: 10.1126/sciadv.aaz5858

The PDF file includes:

Other Supplementary Material for this manuscript includes the following:

(available at advances.sciencemag.org/cgi/content/full/6/22/eaaz5858/DC1)

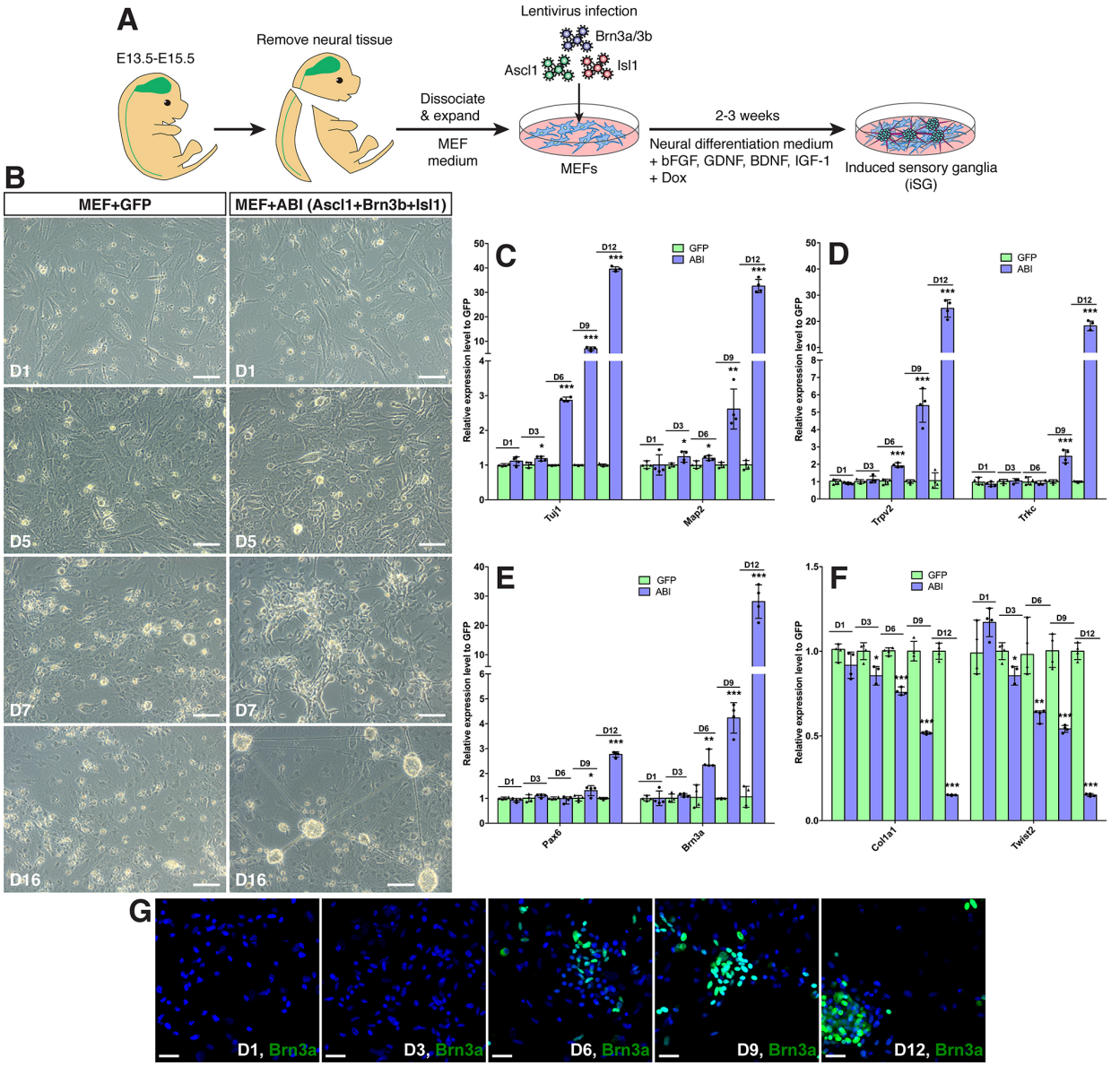

Fig. S1. Generation of induced sensory ganglia (iSG) from mouse embryonic fibroblasts (MEFs) by direct reprogramming with Ascl1, Brn3a/3b and Isl1. (**A**) Schematic of the reprogramming procedure. MEFs were prepared from E13.5-E15.5 C57BL6/J mouse embryos and infected with a mixture of tet-on lentiviruses expressing Ascl1, Brn3a/3b and Isl1. They were induced by doxycycline (dox) and cultured for 2-3 weeks in neural differentiation medium containing bFGF, GDNF, BDNF, and IGF-1 to induce iSG. (**B**) Morphological changes of MEFs infected with GFP lentiviruses or those expressing ABI (Ascl1, Brn3b and Isl1). Cell clusters could be seen in ABI virus-infected MEFs by day (D) 7 in culture, but not in GFP virus-infected MEFs. Many networked iSG were formed in ABI-transduced MEFs by day 16, while in GFP-transduced MEFs, there were none. Scale bars: 80 μm. (**C-E**) qRT-PCR assay showing the time course (D1-D12) of upregulation of the neuron marker genes *Tuj1, Map2, Trpv2, TrkC, Pax6* and *Brn3a* in MEFs infected with ABI viruses, compared to those infected with GFP viruses. Data are presented as mean ± SD (*n*=4). Asterisks indicate significance in unpaired two-tailed Student's t-test: *p<0.05,

p<0.005, ***p<0.0005. (F**) qRT-PCR assay showing the time course (D1-D12) of downregulation of the fibroblast marker genes *Col1a1* and *Twist2* in MEFs infected with ABI viruses, compared to those infected with GFP viruses. Data are presented as mean ± SD (n=4). Asterisks indicate significance in unpaired two-tailed Student′s t-test: *p<0.05, **p<0.005, ***p<0.0005. (**G**) MEFs induced by ABI for the indicated number of days (D) were immunostained with an anti-Brn3a antibody and counterstained with nuclear DAPI. Scale bars: 20 μm.

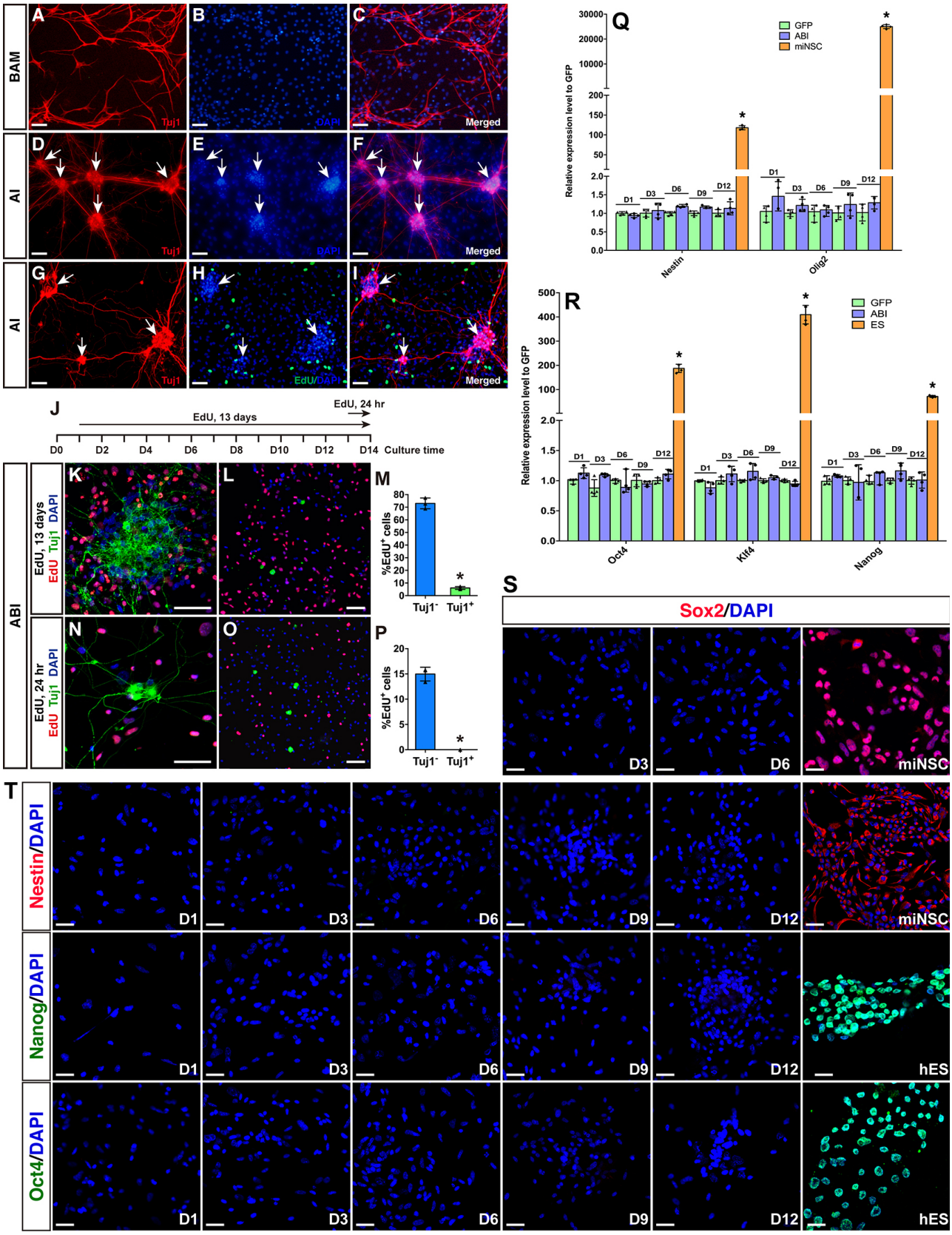

Fig. S2. Induction of iSG by AI or ABI without undergoing a proliferative intermediate state. (**A-C**) Tuj1-immunoreactive iNs induced by BAM from MEFs were scattered and did not form iSG. Scale bars: 40 μm. (**D-F**) Tuj1-immunoreactive iNs induced by AI from MEFs

coalesced into networked and clustered iSG. Arrows point to iSG visualized by Tuj1-immunolabeling and DAPI-labeling. Scale bars: 40 μm. (**G-I**) iNs induced by AI from MEFs were pulse-labeled by EdU for 24 hours prior to fluorescent colabeling for both Tuj1 and EdU. Arrows point to iSG visualized by Tuj1-immunolabeling and DAPI-labeling. Scale bars: 40 μm. (**J**) Schematic of EdU labeling schedule during the ABI reprogramming process. (**K,L**) ABI-transduced MEFs were labeled by EdU for 13 days and colabeled by fluorescence for both Tuj1 and EdU before dissociation (K) and after dissociation (L). Scale bars: 40 μm. (**M**) Quantification of corresponding EdU-labeled cells in populations of Tuj1-negative and Tuj1-positive cells. Data are presented as mean ± SD (*n*=3). The asterisk indicates significance in unpaired two-tailed Student′s t-test: **p*<0.0001. (**N,O**) ABI-transduced MEFs were labeled by EdU for 24 hours and colabeled by fluorescence for both Tuj1 and EdU before dissociation (N) and after dissociation (O). Scale bars: 40 μm. (**P**) Quantification of corresponding EdU-labeled cells in populations of Tuj1-negative and Tuj1-positive cells. Data are presented as mean ± SD (*n*=3). The asterisk indicates significance in unpaired two-tailed Student′s t-test: **p*<0.0001. (**Q**) qRT-PCR assay showing no significant change in expression levels of the neural stem cell marker genes *Nestin* and *Olig2* in MEFs infected with ABI viruses, compared to those infected with GFP viruses, during the time course (D1-D12) of reprogramming. Data are presented as mean ± SD (*n*=4). Asterisks indicate significance in unpaired two-tailed Student′s t-test: **p*<0.0001. A mouse neural stem cell (miNSC) line was used as a positive control. (**R**) qRT-PCR assay showing no significant change in expression levels of the pluripotent factor genes *Oct4, Klf4* and *Nanog* in MEFs infected with ABI viruses, compared to those infected with GFP viruses, during the time course (D1-D12) of reprogramming. Data are presented as mean ± SD (*n*=4). Asterisks indicate significance in unpaired two-tailed Student′s t-test: **p*<0.0001. A mouse embryonic stem cell (ES) line was used as a positive control. (**S,T**) MEFs induced by ABI for the indicated number of days (D) were immunostained with antibodies against the neural stem cell and/or pluripotent stem cell markers Sox2, Nestin, Nanog or Oct4 and counterstained with nuclear DAPI. A mouse neural stem cell (miNSC) line was used as a positive control for Sox2 and Nestin and an embryonic stem cell (hES) line was used as a positive control for Nanog and Oct4. Scale bars: 20 μm.

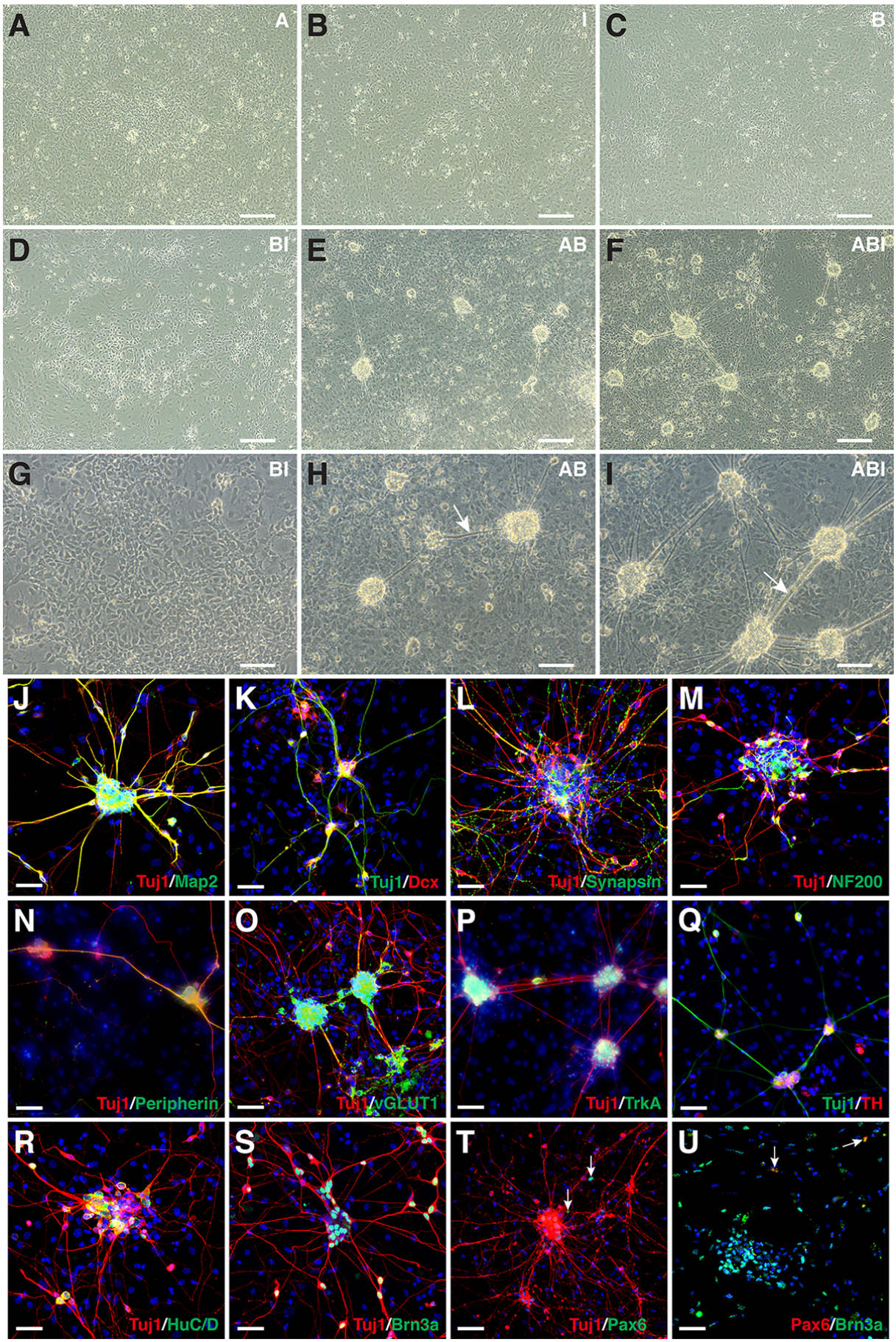
A
A
B
I
C
B
D
BI
E
AB
F
ABI
G
BI
H
AB
I
ABI
J
Tuj1/Map2
K
Tuj1/Dcx
L
Tuj1/Synapsin
M
Tuj1/NF200
N
Tuj1/Peripherin
O
Tuj1/vGLUT1
P
Tuj1/TrkA
Q
Tuj1/TH
R
Tuj1/HuC/D
S
Tuj1/Brn3a
T
Tuj1/Pax6
U
Pax6/Brn3a

Fig. S3. Induction of iSG from MEFs by direct reprogramming with Ascl1, Brn3a and Isl1 (ABI) and characteristics of iSG and iRGCs reprogrammed by AI. (**A-I**) Morphological changes of MEFs infected with the indicated lentiviruses (A, Ascl1; B, Brn3a; I, Isl1) and cultured for 14 days. Networked iSG were induced by combinations of Ascl1 with Brn3a (AB) or both Brn3a and Isl1 (ABI), with the ABI triple factor combination as more effective. Arrows point to the thick fasciculated nerve fibers interconnecting iSG. Scale bars: 160 μm (A-F) and 80 μm (G-I). (**J-U**) MEFs were infected with the AI lentiviruses, cultured for 14 days, and then double-immunostained with the indicated antibodies and counterstained with nuclear DAPI. iSG induced by AI were immunoreactive for Tuj1, Map2, Dcx, synapsin, NF200, peripherin, vGLUT1, TrkA, TH, HuC/D, or Brn3a. iRGCs immunoreactive for Pax6 or both Brn3a and Pax6 (indicated by arrows) were few and distributed outside the iSG. Scale bars: 40 μm.

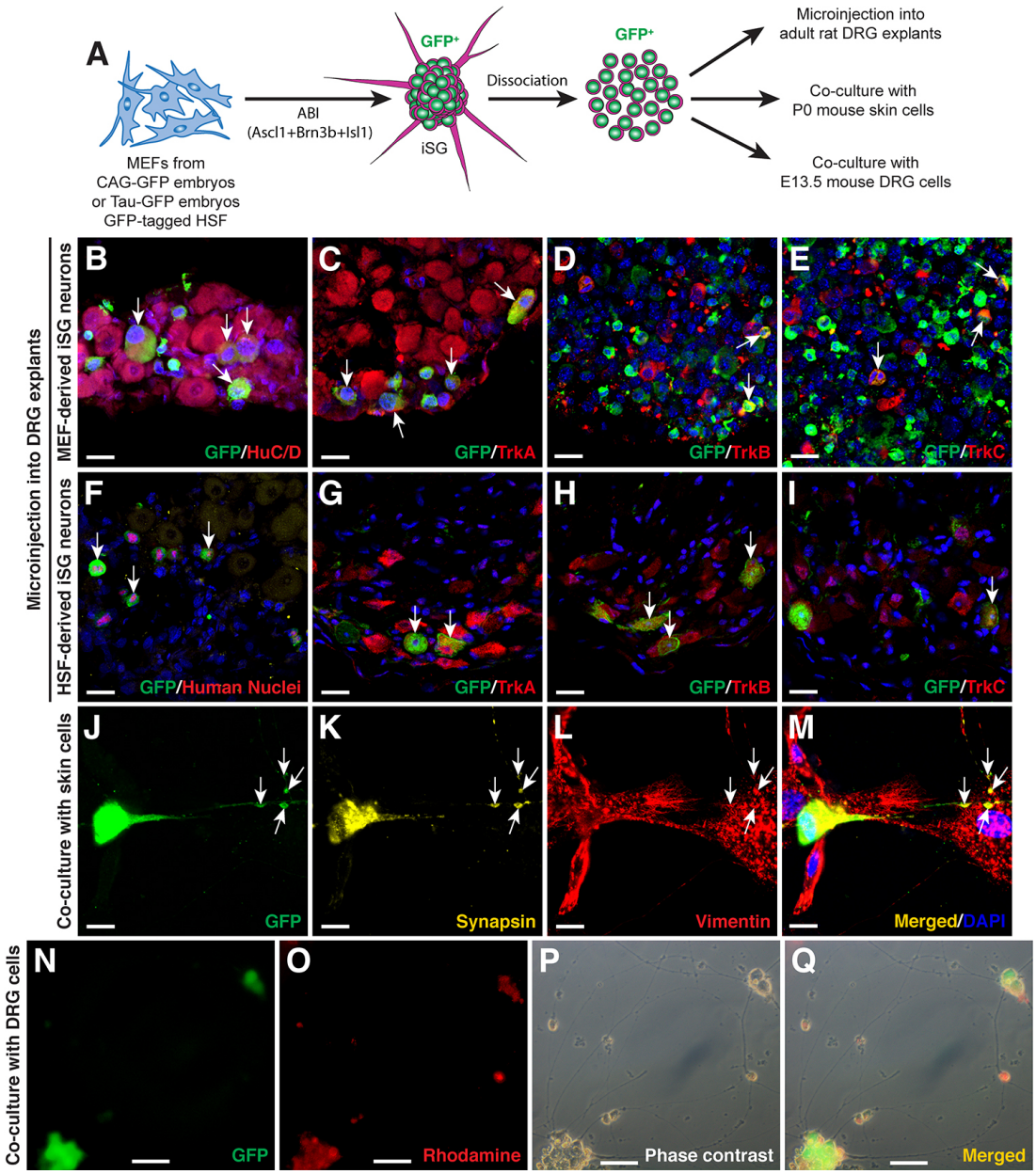

Fig. S4. DRG integration and epidermal cell innervation by iSG neurons. (**A**) Schematic of the integration and co-culture experiments. (**B-E**) Two weeks after CAG-GFP-tagged iSG neurons were microinjected into adult rat dorsal root ganglion (DRG) explants, the grafted explants were double-immunostained with the indicated antibodies and counterstained with nuclear DAPI. Arrows point to representative double-positive cells. Scale bars: 20 μm. (**F-I**) Two weeks after HSF (human skin fibroblast)-derived GFP-tagged iSG neurons were microinjected into adult rat DRG explants, the grafted explants were double-immunostained with the indicated antibodies and counterstained with nuclear DAPI. Arrows point to representative double-positive cells. Scale bars: 20 μm. (**J-M**) Tau-GFP-tagged iSG neurons were dissociated and co-cultured with dissociated P0 mouse skin cells for one week, then triple-immunostained with the indicated antibodies and counterstained with nuclear DAPI. Arrows indicate multiple nerve endings extended from the iSG neuron. Scale bars: 12.7 μm. (**N-Q**) Tau-GFP-tagged iSG neurons were dissociated and co-cultured with rhodamine-labeled E13.5 mouse DRG cells for one week, then immunostained with an anti-GFP antibody. iSG neurons were seen to co-aggregate with DRG cells. Scale bars: 160 μm.

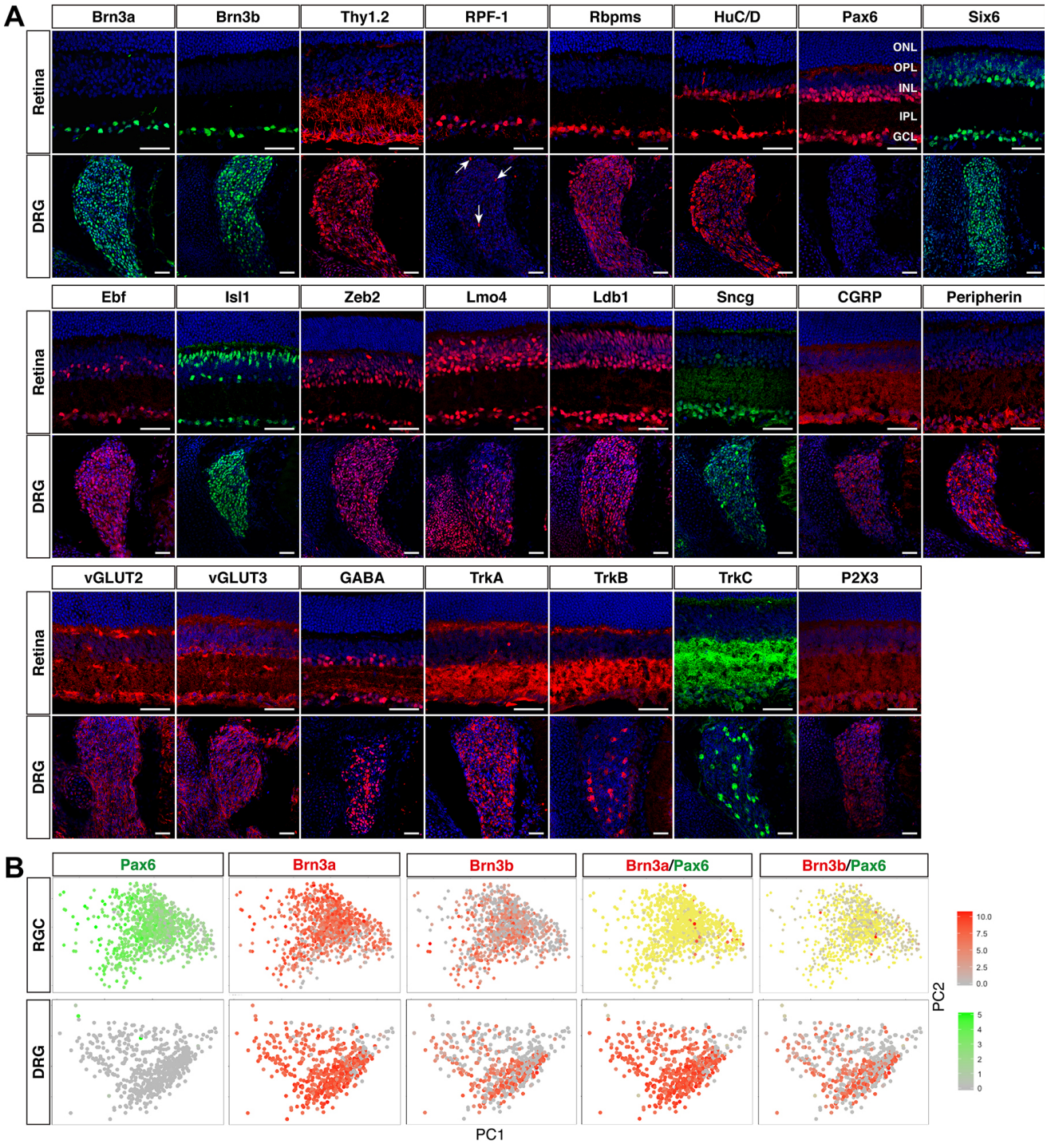

Fig. S5. Expression specificity of a series of commonly used RGC and sensory neuron markers in the retina and dorsal root ganglion (DRG). (**A**) P21 mouse retinal sections and E13.5 DRG sections were stained by immunofluorescence with the indicated antibodies and counterstained with nuclear DAPI. It appears that all commonly used "RGC-specific" markers (e.g. Brn3a, Brn3b, Thy1.2, RPF-1, Rbpms, and Sncg) are expressed in the DRG. Pax6, which is expressed in RGCs but not RGC-specific, is the only tested protein marker that exhibits no expression in the DRG. Arrows point to DRG neurons immunoreactive for RPF-1. Abbreviations: GCL, ganglion cell layer; INL, inner nuclear layer;

IPL, inner plexiform layer; ONL, outer nuclear layer; OPL, outer plexiform layer. Scale bars: 40 μm. (**B**) Relative expression levels of *Pax6, Brn3a* and *Brn3b* genes in RGCs and DRG cells as determined by single cell RNA-seq profiling. *Brn3a*$^{+}$*Pax6*$^{+}$ and *Brn3b*$^{+}$*Pax6*$^{+}$ double-positive cells are abundant in RGCs but absent from the DRG. The principal components PC1 and PC2 are plotted and the relative expression levels are indicated by colors.

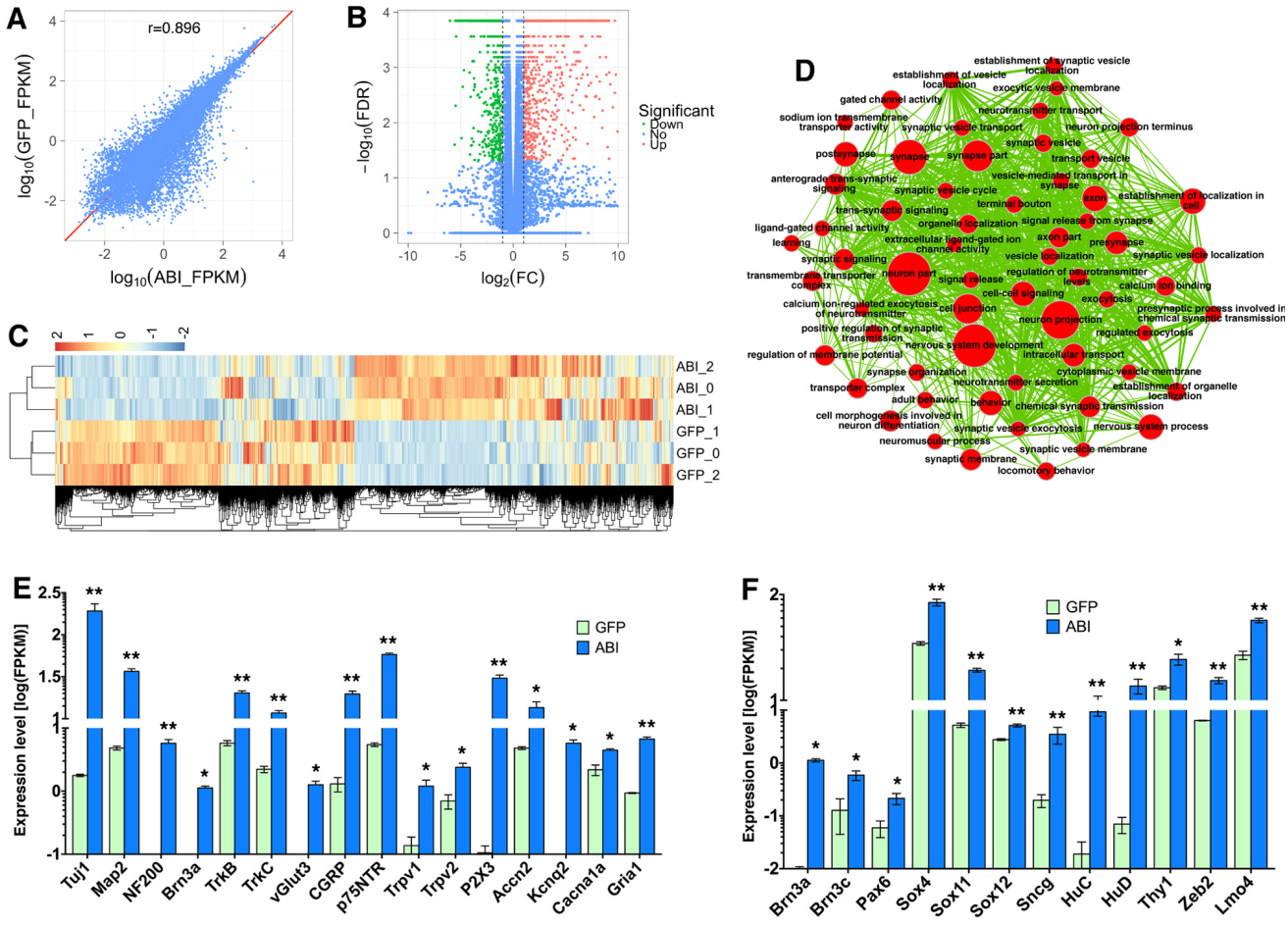

Fig. S6. Global gene expression profiles of MEFs infected by GFP lentiviruses or ABI lentiviruses determined by bulk RNA-seq analysis. (**A**) Scatter plot analysis of the global gene expression profiles of GFP-transduced and ABI-transduced MEFs. Gene expression levels (FPKM) are depicted in $\log_{10}$ scale. The Pearson correlation coefficient (r) is indicated. (**B**) Volcano plot (significance vs fold change) of significantly altered genes (fold change ≥ 2 and FDR < 0.05) between GFP-transduced and ABI-transduced MEFs. (**C**) Heat map of the z-transformed gene expression values in GFP-transduced and ABI-transduced MEFs. (**D**) Gene ontology (GO) enrichment analysis of the upregulated genes between GFP-transduced and ABI-transduced MEFs. The upregulated genes were analyzed for GO term enrichment by gene set enrichment analysis (GSEA). The result was visualized on a network of gene-sets (nodes) connected by their similarity (edges). Node size represents the gene-set size and edge thickness represents the degree of overlap between two gene sets. (**E**) Expression levels [log(FPKM)] of the indicated significantly upregulated genes in ABI-transduced compared to GFP-transduced MEFs, which represent general and subtype-specific sensory neuron markers. Data are presented as mean ± SD (*n*=3). Asterisks indicate significance in unpaired two-tailed Student's t-test: **p*<0.005, ***p*<0.0001. (**F**) Expression levels (log(FPKM)] of the indicated significantly upregulated genes in ABI-transduced compared to GFP-transduced MEFs, which represent RGC-related markers. Data are presented as mean ± SD (*n*=3). Asterisks indicate significance in unpaired two-tailed Student's t-test: **p*<0.05, ***p*<0.0005.

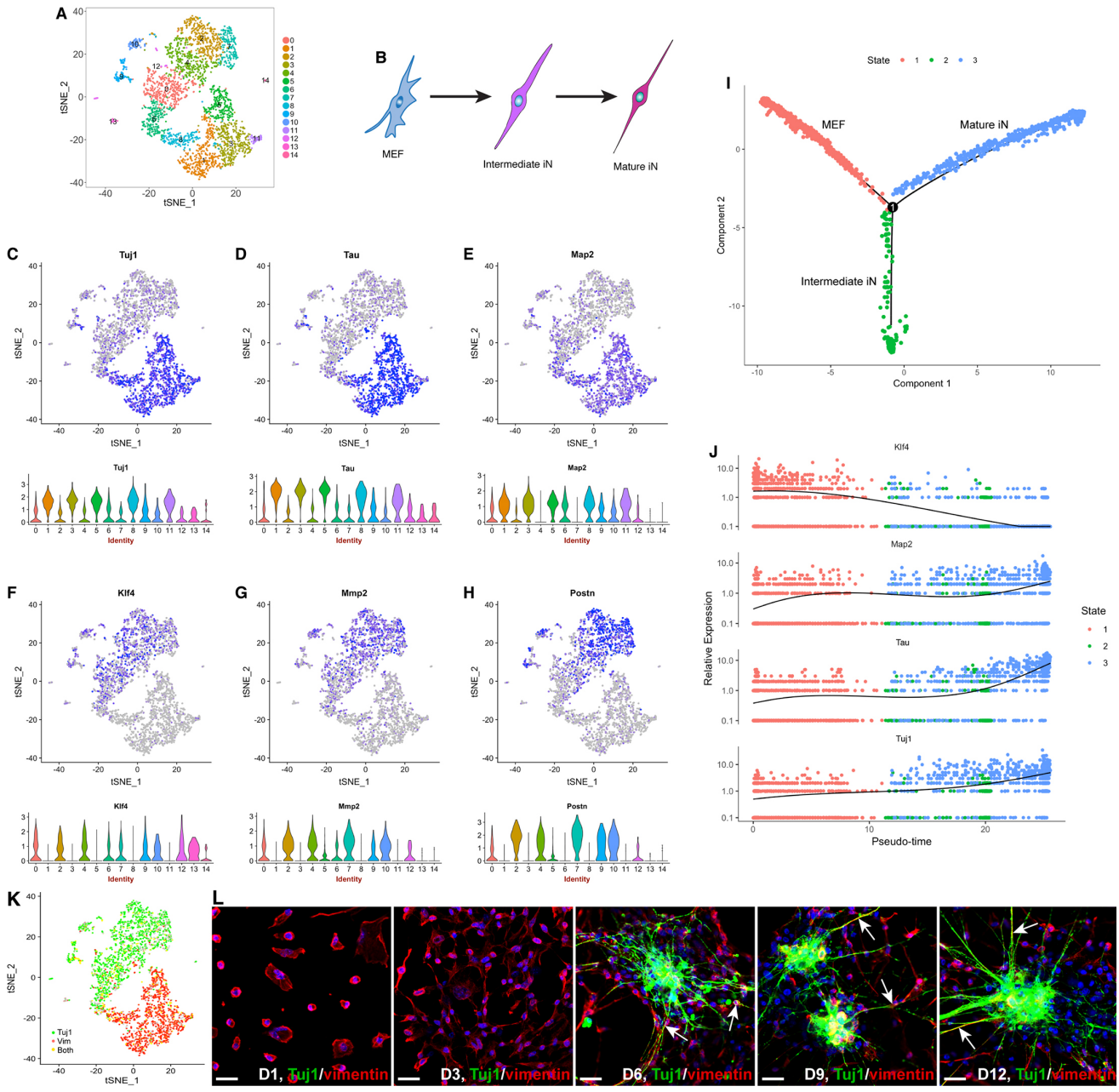

Fig. S7. MEFs undergo an intermediate stage before reprogrammed by ABI into mature iSG neurons. (**A**) t-SNE plot of the 15 iSG cell clusters. (**B**) Schematic illustration of the cellular stages during the ABI-mediated reprogramming process. (**C-E**) t-SNE plots colored by expression of the indicated neuronal marker genes and corresponding violin plots showing their expression in iSG cell clusters. (**F-H**) t-SNE plots colored by expression of the indicated MEF marker genes and corresponding violin plots showing their expression in iSG cell clusters. (**I**) A pseudotime trajectory of the sequenced cells constructed using Monocle. Indicated in color are the three presumptive states and corresponding cell population. (**J**) Relative expression levels of *Klf4, Map2, Mapt* and *Tuj1* in pseudotime. (**K**) t-SNE plots colored by expression of *Tuj1* and *Vim* (*vimentin*) genes. (**L**) MEFs induced by ABI for the indicated number of days (D) were double-immunostained with antibodies against Tuj1 and vimentin and counterstained with nuclear DAPI. Arrows point to representative colocalized cells or nerve bundles. Scale bars: 20 μm.

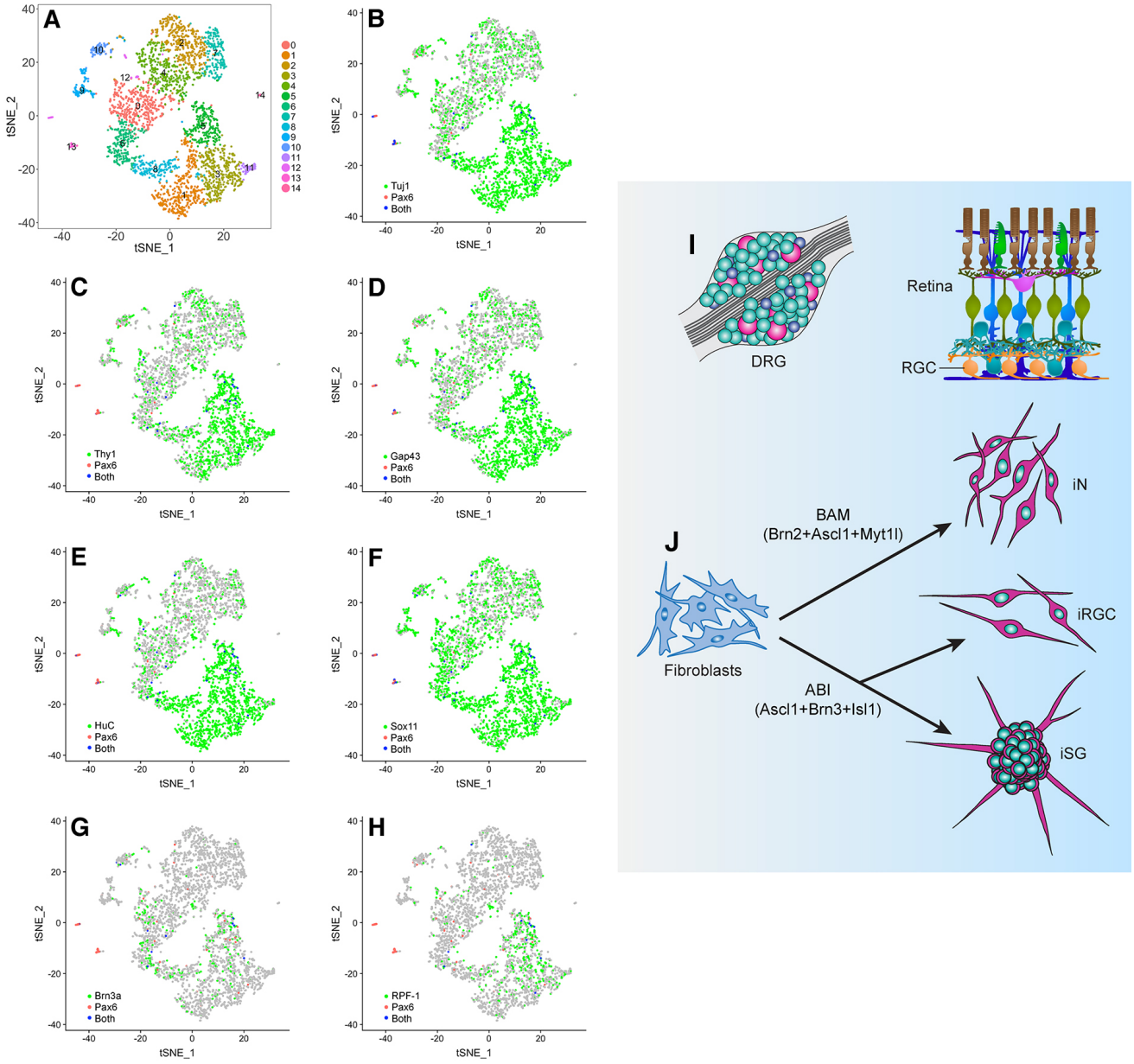

Fig. S8. Morphologically distinct iSG and iRGCs reprogrammed from fibroblasts by ABI. (**A**) t-SNE plot of the 15 iSG cell clusters. (**B-H**) t-SNE plots colored by expression of *Pax6* and the indicated conventional RGC marker genes. (**I**) Schematic of the DRG and retina. Compared to the clustered sensory neurons in the DRG, RGCs do not form a cluster but instead widely spread in a layer with a single-cell thickness (RGC layer) in the retina. (**J**) Schematic indicating the outcome of fibroblasts induced by BAM or ABI. ABI-reprogrammed iSG and iRGCs morphologically resemble DRG and retinal RGCs, respectively.

Other Supplementary Material for this manuscript:

Table S1 (Microsoft Excel format). List of genes differentially expressed between ABI-transduced and GFP-transduced MEFs as determined by RNA-seq analysis.

Table S2 (Microsoft Excel format). Gene-specific primers used for qRT-PCR analyses.

Videos S1 and S2. MEFs prepared from the CAG-GFP transgenic mouse embryos were induced by ABI (Ascl1, Brn3b and Isl1) for 10 days, then recorded by long-term time-lapse microscopy. Videos S1 and S2 are simultaneous fluorescent and phase-contrast recordings of the same field, respectively, showing how individual neurons induced by ABI self-organized into an iSG.

Videos S3 and S4. MEFs prepared from the CAG-GFP transgenic mouse embryos were induced by A (Ascl1) for 10 days, then recorded by long-term time-lapse microscopy. Videos S3 and S4 are simultaneous fluorescent and phase-contrast recordings of the same field, respectively, showing no self-organization of induced neurons.